FIRST PRINCIPLES CALCULATION OF CHARGED VACANCY DIFFUSION IN NICKEL OXIDE

by

Hanju Sun

B.S. in Material Forming and Control Engineering, Northwestern Polytechnical University,

2013

Submitted to the Graduate Faculty of

Swanson School of Engineering in partial fulfillment

of the requirements for the degree of

Master of Science

University of Pittsburgh

2016

UNIVERSITY OF PITTSBURGH

SWANSON SCHOOL OF ENGINEERING

This thesis was presented

by

Hanju Sun

It was defended on

March 25, 2016

and approved by

Guofeng Wang, PhD, Associate Professor, Department of Mechanical Engineering and Material Science

Sangyeop Lee, PhD, Assistant Professor, Department of Mechanical Engineering and Material Science

Scott X. Mao, PhD, Professor, Department of Mechanical Engineering and Material Science

Thesis Advisor: Guofeng Wang, PhD, Associate Professor, Department of Mechanical Engineering and Material Science

FIRST PRINCIPLES CALCULATION OF CHARGED VACANCY DIFFUSION IN NICKEL OXIDE

Hanju Sun, M.S.

University of Pittsburgh, 2016

We studied the diffusion of charged vacancies in nickel oxide (NiO) crystal using the first-principles calculation method. We determined the formation energy and migration energy of vacancies with various charge states in NiO. Detailed diffusion paths on atomic scale of various charged vacancies in NiO crystal were investigated. Further analysis about physical origin of charge-dependent vacancy diffusion has been done. Our results reveal that the number of electrons occupying defect level and defect level shift have an important impact on migration energy of the vacancy, especially for charged O vacancies in intrinsic NiO crystal.

TABLE OF CONTENTS

LIST OF TABLES

LIST OF FIGURES

ACKNOWLEDGMENT

I am very grateful to my advisor, Dr. Guofeng Wang. He provides the device and software license so that I can do this research. Moreover, I thank the members of his group, especially, Yingkai Lei, Zhenyu Liu and Kexi Liu for giving a lot of help to my thesis.

I express my gratitude to my thesis committee members, Dr. Scott X. Mao, Dr. Sangyeop Lee, for their attention and patience.

1.0 INTRODUCTION

Nickel is commonly used in high temperature alloys [1] and stainless steels [2] as a base element or an added element. When alloys are employed in high-temperature oxidation environments, they are protected by oxide scale. The requirements for good protection in long period are that the growth of oxide scale should be sufficient slow and the oxide scale should not spall or crack to re-expose the underlying metal [3]. In long period, the growth of the compact oxide scale is diffusion-limited. Knowledge about vacancy diffusion in NiO crystal will contribute to investigations of the growth of oxide scales on nickel alloys during high-temperature oxidation.

NiO is a sodium-chloride-structured oxide from room temperature to its melting point. NiO is antiferromagnetic below its Néel temperature (525K). Planes of spin-up and spin-down sites are stacked in an alternating manner along the [111] direction (as shown in Fig.1). For most situations, the primary defects in NiO are cation vacancies and electron holes [4]. Stoichiometry studies of NiO [5, 6] show excess oxygen ions than nickel ions. In addition, the self-diffusion of cation [7] is much more rapid than self-diffusion of onion [8] in NiO, which suggest the excess oxygen ions are accommodated by the formation of cation vacancies and electron holes rather than by the formation of interstitial anions [9].

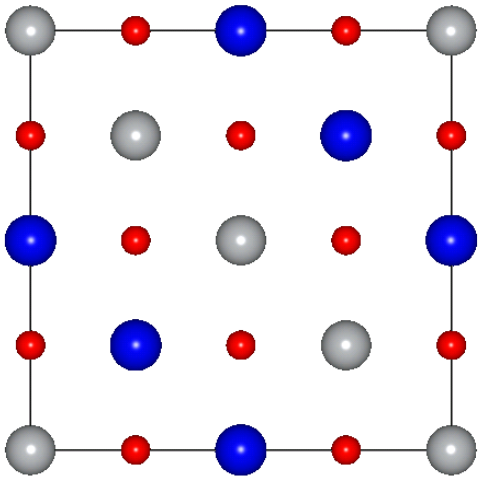

Figure 1. Schematic view of the central layer of the supercell which corresponds to a [100] plane of NiO. Big balls represent Ni atoms, while additionally the spin-up and spin-down are marked with gray and blue. Red small balls represent O atoms.

In previous work, the chemical-diffusion coefficient of NiO was generally measured through thermogravimetric techniques and electrical conductivity [10-12]. According to Arrhenius plot with the logarithm of diffusion coefficient as a function of the reciprocal of temperature and equation:

$$D = f\ exp(\frac{-\Delta E}{kT}) \quad (1)$$

, the activation energy and prefactor can be deduced. In the equation above, D is diffusion coefficient, ΔE is activation energy and f is prefactor. However, deep discussion of vacancy charge effect on diffusion barrier was seldom reminded. Detailed diffusion path on atomic scale has not been investigated. In my thesis, we try to figure out the physical origin of the charge-

dependent vacancy diffusion and detailed diffusion paths in NiO with the first-principles density functional theory plus U (DFT+U) method.

2.0 BACKGROUND

2.1 DIFFUSION IN NIO

2.1.1 Experimental researches

Most of researches on diffusion in NiO crystal were done through experimental methods. Diffusion coefficient of Ni and O in NiO crystal are most concerned. Since the major defect in NiO crystal are Ni vacancies and electron holes, the researches on Ni diffusion are much more than O diffusion in NiO crystal. However, Several authors suggested that diffusion of oxygen may be a contributing mechanism in the growth of oxide films on nickel [13]. Tracer method [3] and surface-activity method [7] were used to measure diffusion coefficient of Ni in NiO crystal. Peterson *et al.* [9] developed a model which was fit to the electrical-conductivity data [11], the deviation-from-stoichiometry data [6] and the cation-self-diffusion data [14, 15]. Diffusion of Ni atoms in the single crystal and along grain boundary were both investigated. But the conclusions deduced by different researchers varies. Shim *et al*. [7] demonstrated that grain-boundary diffusion did not play any important part either in the observed diffusion of radioactive nickel or in the parabolic nickel oxidation. While Atkinson *et al*. [16] measured the width of the grain boundary to be 7×10^{-8} cm and found that in this region near the boundary the concentration and mobility of Ni vacancies were greater than in the bulk. Atkinson *et al*. concluded that the measured values of grain boundary width confirmed quantitatively that the

rate of oxidation of Ni to NiO at 500–800 ℃ was controlled by the diffusion of Ni along grain boundaries in the NiO scale. The different conclusion may due to different temperatures. Shim's experiments were carried out from 1000 to 1400°C in air while Atkinson's measurements were made at an oxygen pressure of 1 atm in a temperature range from 500 to 800 ℃.

2.1.2 Computational researches

Compared with experiment methods, computational methods have several advantages such as low-cost and scalability and several disadvantages such as instability. So computational methods and experiment methods can be used as a supplement and proof for each other.

Molecular dynamics (MD) is a computational simulation method for studying the physical movements of atoms and molecules. Garruchet *et al*. performed variable charge molecular dynamics to study the diffusion mechanisms of oxygen atoms in nickel in a temperature range from 950 K to 1600 K. Garruchet *et al*. observed that oxygen did not diffuse via jumps of oxygen through interstitial sites but via a vacancy diffusion mechanism.

Density functional theory (DFT) is a first-principle calculation method. By solving the basic equations of quantum mechanics, DFT method would determine the properties of the materials. Due to the convenience of constructing structures by DFT methods, most DFT calculations which were done to study diffusion problems were performed on more complex systems which corresponded to situations in reality to obtain data or predict phenomena. While the DFT calculation on vacancy diffusions in intrinsic NiO crystal which aimed to reveal some physical origin of diffusion was seldom performed. Detailed diffusion paths of Ni vacancies and O vacancies on atom scale in intrinsic NiO crystal have not been investigated.

Monte Carlo methods are a broad class of computational algorithms that rely on repeated random sampling to obtain numerical results, which is suitable to be used to simulate the diffusion process of vacancies with various configurations and charge states. Babak Sadigh *et al*. [17] combined first-principle calculation and Kinetic Monte Carlo simulation to study the mechanism of boron diffusion in silicon.

2.2 DENSITY FUNCCTIONAL THEORY

Density functional theory (DFT) is a first principles or ab initio method based on quantum mechanics used to investigate the electronic structure (principally the ground state) of many-body systems, in particular atoms, molecules, and the condensed phases. In many cases the results of DFT calculations for solid-state systems agree quite satisfactorily with experimental data. Due to its good accuracy and efficiency, it is increasingly being used in physics, chemistry, material science, biochemistry and many branches of engineering. For example, DFT has been used to illuminate that defects promote the reactivity for epoxidation of propylene in titanosilicate (TS-1) catalysts [18] and the impact of vacancies and holes on the fracture of carbon nanotube [19]. Despite the development and improvement of DFT in recent years, there are still difficulties in using DFT to properly describe intermolecular interactions, especially in calculations of the band gap and ferromagnetism in semiconductors [20]. Although DFT is much more efficient than traditional methods such as Hartree–Fock theory and its descendants based on the complex many-electron wavefunction, Computational costs rise distinctly with increasing the number of atoms. Therefore, it is not suggested to use DFT in a system containing more than 100 atoms now. However, with the development of computer

science and improvement of approximation methods of DFT, the limit of the number of atoms will be broken into a larger scale. A brief overview of the fundamentals of density functional theory is illustrated below.

2.2.1 Schrödinger's equation

Analogous to Newton's law for classical mechanics, Schrödinger's Equation is used to describe the change of quantum system with time in quantum mechanics. Since the mass of a proton or neutron is about 1800 times greater than an electron, the nuclei of the treated molecules or clusters are seen as fixed and only electrons moves as usual in many-body electronic structure calculations. According to Born–Oppenheimer (BO) approximation [21], the motion of atomic nuclei and electrons in a molecule can be separated. Then the Schrödinger's Equation can be simplified as time-independent:

$$\hat{\mathrm{H}}\Psi = E\Psi \tag{1}$$

where Ψ is the electronic wave function describing the stationary electronic state and E is the total energy. According to Hohenberg–Kohn theorems [22], for a system with N electrons and k nuclei, the Hamiltonian, $\hat{\mathrm{H}}$, is defined as the following equation:

$$\hat{\mathrm{H}} = -\frac{\hbar^2}{2m_e}\sum_{i=1}^{N} v_i^2 + \sum_{i=1}^{N}\sum_{j=1}^{k} V_j(r_i) + \frac{1}{2}\sum_{i=1}^{N}\sum_{j\neq i}^{N}\frac{e^2}{|r_i - r_j|} \tag{2}$$

The terms in the Hamiltonian represent the kinetic energy of electrons, the interaction energy between each electron and all nuclei, and the interaction energy between electrons, respectively.

2.2.2 Exchange-correlation functional

Exchange-correlation functional, $E_{xc}[n(r)]$, accounts for the difference between the exact ground-state energy and the energy calculated by the Hartree approximation. However, the exact form of E_{xc} is still unknown and may never be known in a closed mathematical form. Thus some sort of approximations for E_{xc} are required. There are two common approximations (in various forms) in use: the local density approximation (LDA) [23], and the generalized gradient approximation (GGA) [24].

The simplest approximation is the LDA which assumes that the exchange-correlation energy at a point is simply equal to the exchange-correlation energy of a uniform electron gas that has the same density at the point as shown in the equation below:

$$E_{ex}^{LDA} = \int n(r) e_{xc}[n(r)] dr \tag{3}$$

where $e_{xc}[n(r)]$ is the exchange-correlation energy per particle of a homogeneous electron gas of density $n(r)$.

Strictly speaking, the LDA is valid only for slowly varying densities. While empirically, LDA in general can also be applied in the system of atoms, molecules, and solids. In addition, LDA works very well for metals. However, recent studies have shown that LDA tends to overestimate cohesive energies by 15-20% and underestimates lattice constants by 2-3% for metals and insulators [25-27].

Compared with LDA, GGA takes account of the gradient of the electron density $\nabla n(r)$ at the same coordinates as shown in the equation below:

$$e_{xc}(r) = e_{xc}[n(r), \nabla n(r)] \tag{4}$$

GGA is better at dealing with the rapidly varying electron densities such as surface, an insulated molecular or atom than LDA. Experiences have shown that GGA is more accurate than LDA, but it often underestimates energies, and results in overestimate lattice parameters. Unlike LDA, GGA functional is not well defined. The most common used GGA functional are the Perdew-Burke-Ernzerhof (PBE) functional [28] and Perdew-Wang (PW91) functional [29].

2.2.3 Pseudopotentials

As we know, most physically interesting properties of solids are largely determined by the valence electrons rather than the core electrons. Then pseudopotential is used to replace the Coulomb potential of the nuclei and the effect of tightly bound core electrons by an effective potential acting on the valence electrons. The model is simplified as a frozen core and valence electrons. The computation cost is dramatically reduced. There are three major kinds of pseudopotentials: norm-conserving pseudopotentials (NCPP), ultrasoft pseudopotentials (USPP), and projector augmented wave (PAW) pseudopotentials. NCPP is rarely used todays, and PAW is the most common used one. USPP can be used to speed up calculation, and for many system, the results calculated by USPP are similar to the result calculated by PAW. PAW is the most accurate in these three, and it gives reliable results in most systems including systems with strong magnetic moments or large difference in electronegativity.

2.2.4 DFT+U

Both LDA and GGA introduce an electron self-interaction energy error. When the on-site Coulomb interaction of localized electrons is strong, the error can not be canceled out. In

transition metal oxide such as nickel oxide, the on-site Coulomb interactions are particularly strong for localized d and f electrons, which introduces an unneglectable error for many properties such as band gap. DFT+U is a simple and efficient method to fix this problem. In this method, a strong intra-atomic interaction in a Hartree-Fock like manner is introduced to describe the strength of on-site Coulomb and exchange by parameters, U and J. The two main branches of DFT+U correction are the one introduced by Liechtenstein et al. [30], in which U and J enter as independent corrections in the calculations, and the one proposed by Anasimov et al. [31], where only a single effective $U_{eff} = U - J$ parameter accounts for the Coulomb interaction, neglecting any higher multi-polar terms. DFT+U method would give correct magnetic ground states, electronic structure for systems and redox reaction energies in oxides [32]. The parameter U is essential for the correction, which will influence the result dramatically. One method to determine the parameter U is through ab initio self-consistent calculation of the given system [33]. But a more commonly used method is fitting parameter U by experimental data on the properties interested.

3.0 VACANCY FORMATION ENERGY

3.1 COMPUTAION METHOD

In this study, the formation energy and diffusion barrier of charged vacancies in NiO were calculated by DFT+U calculations. The projector augmented wave method [34] and the Perdew-Burke-Ernzerhof exchange-correlation functional [28] which are implemented in the Vienna Ab initio Simulation Package (VASP) [35, 36] were chosen in this study. A kinetic energy cutoff of 600 eV was used in all these calculation. The NiO bulk crystal was modeled with a 2×2×2 supercell of conventional face-centered cubic cell lattice (shown in Fig. 2). Without vacancy defects, there are 32 Ni atoms and 32 O atoms in total in our simulation cell. A 3×3×3 Monkhorst-Pack k-point mesh [37] for k-points mesh integration was used in our DFT+U calculation. An effective interaction parameter $U_{eff} = U - J = 6.4eV$ was selected as suggested in Ref. [38].

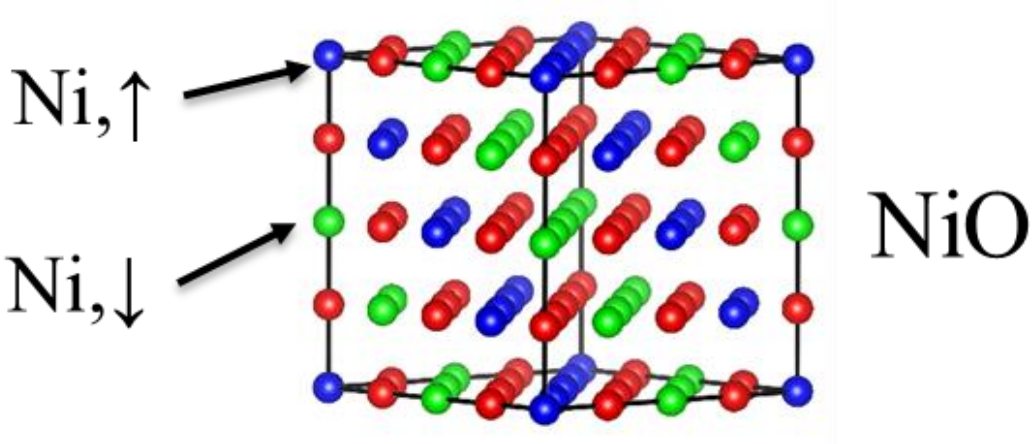

Figure 2. 2×2×2 supercell of bulk NiO crystal with conventional face-centered cubic cell lattice. In the figure, the red balls represent O atoms, the blue balls represent Ni atoms with spin up and the green balls represent Ni atoms with spin down.

A vacancy was achieved by removing a relevant atom and changing the total number of electrons corresponding to the charge of the vacancy. The formation energy and mobility of the Ni vacancy with a 0 (V_{Ni}^{0}), -1 (V_{Ni}^{1-}) or -2 (V_{Ni}^{2-}) charge and the O vacancy with a 0 (V_{O}^{0}), +1 (V_{O}^{1+}) or +2 (V_{O}^{2+}) are considered in this study. Except the transition state structure of O vacancy with 0 charge (V_{O}^{0}) was optimized under constant-volume restriction until the Hellman-Feynman force exerted on each ion is less than 0.05 eV/Å. All crystal structures here were optimized under Hellman-Feynman force limitation of 0.01 eV/Å

The vacancy formation energy (ΔE_f) with q charges in NiO was evaluated from this equation [39]:

$$\Delta E_f = E^{def,q} - E^{perf} + \mu_i + q\mu_e \quad (5)$$

where $E^{def,q}$ denote the energy of the relaxed simulation cell containing the charged vacancy and E^{perf} is the energy of the perfect crystal; μ_i is the chemical potential of the removed Ni or O atom from NiO crystal; μ_e is the chemical potential of an electron in NiO. While calculating

$E^{def,q}$, we used Freysoldt, Neugebauer and Van de Walle (FNV) correction [40] to eliminate the finite size error generated by periodic charges. As for chemical potential, μ_i is calculating following the scheme suggested in Ref. [39] and using experiment data [41] and DFT result as inputs; μ_e was calculated as a summation of the valence-band maximum (E_{VBM}) of the perfect crystal and a Fermi level ε_F (whose value is zero at VBM). E_{VBM} was taken as an energy difference between the bulk NiO with 0 and 1+ charge and ε_F was calculated through satisfying the requirement of charge neutrality in the crystal.

3.2 RESULTS AND DISCUSSION

As shown in Fig. 3 and Table. 1, $U_{eff} = 6.4\ eV$ effectively corrects the band gap error in the NiO crystal.

Table 1. Calculated lattice parameter and band gap of NiO crystal by DFT and DFT+U method. Experiment data are also presented for comparison.

	DFT	**DFT+U**	**Experiment**
Lattice parameter	4.198	4.198	4.171 [42]
Band gap	0.77	3.4	3.4~4.3 [43-45]

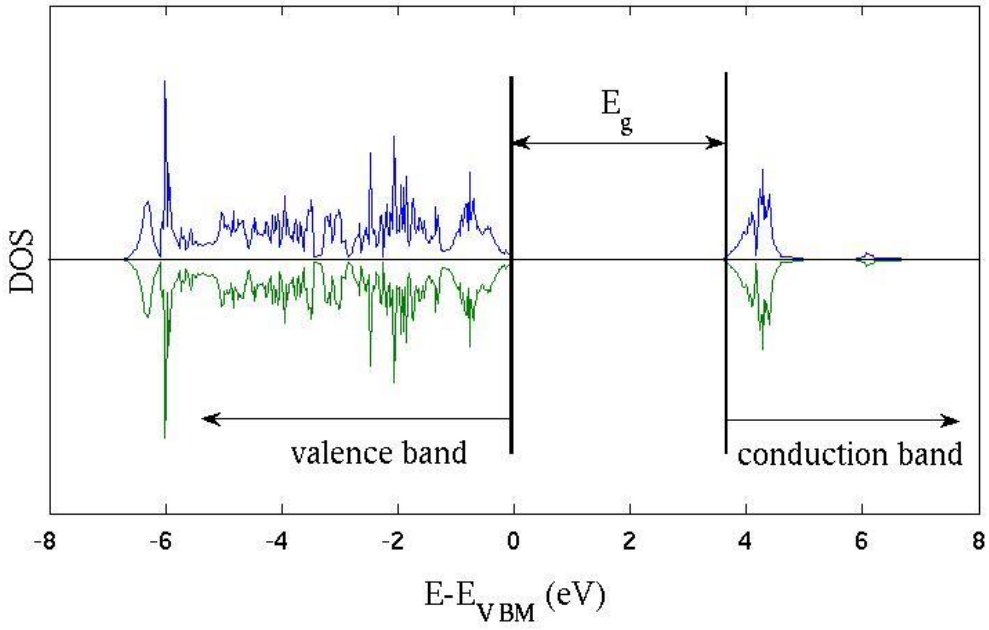

Figure 3. The DOS of perfect NiO crystal with U_{eff} = 6.4 eV

It should be pointed out that the Fermi level ε_F of NiO crystal influences the stability of charged vacancies and can be adjusted through changing the concentration of aliovalent dopants. At the no doping particles condition, we found from our DFT calculation results that V_{O}^{0} would be the most stable O vacancy when ε_F is greater than 1.18 eV, V_{O}^{1+} would be the most stable O vacancy when ε_F is between 0.98 eV and 1.18 eV and V_{O}^{2+} would be the most stable O vacancy when ε_F is below 0.98 eV. As for charged Ni vacancies, the DFT calculation results showed that the stable region of ε_F for V_{Ni}^{0}, V_{Ni}^{1-} and V_{Ni}^{2-} was from 0.0 eV (i.e., EVBM) to 0.56 eV, from 0.56 eV to 0.95 eV and greater than 0.95 eV, respectively. It should be reminded that the overbinding of GGA in the O_2 molecule could result in underestimation of the formation energy of O vacancies. Thus, our DFT predictions on the stability of charged O vacancies and charged Ni vacancies are qualitative (not quantitative). Take an example at

condition of T=1000 K and p_{O_2} =0.2 atm, as shown in Fig. 4, ε_F is 1.70 eV in the calculation result of an un-doped NiO crystal. The most stable vacancies in intrinsic NiO crystal are predicted to be V_{Ni}^{2-} for Ni vacancies and V_{O}^{0} for O vacancies at this condition. P-type doping in NiO crystal will lead to a decrease in ε_F, which makes V_{Ni}^{0}, V_{Ni}^{1-}, V_{O}^{1+} and V_{O}^{2+} more likely to occur. The result of vacancy formation energies of Ni vacancies and O vacancies with different charge states at this condition is shown in Table. 2. This result is also in qualitative nature due to the overbinding of GGA in the O_2 molecule.

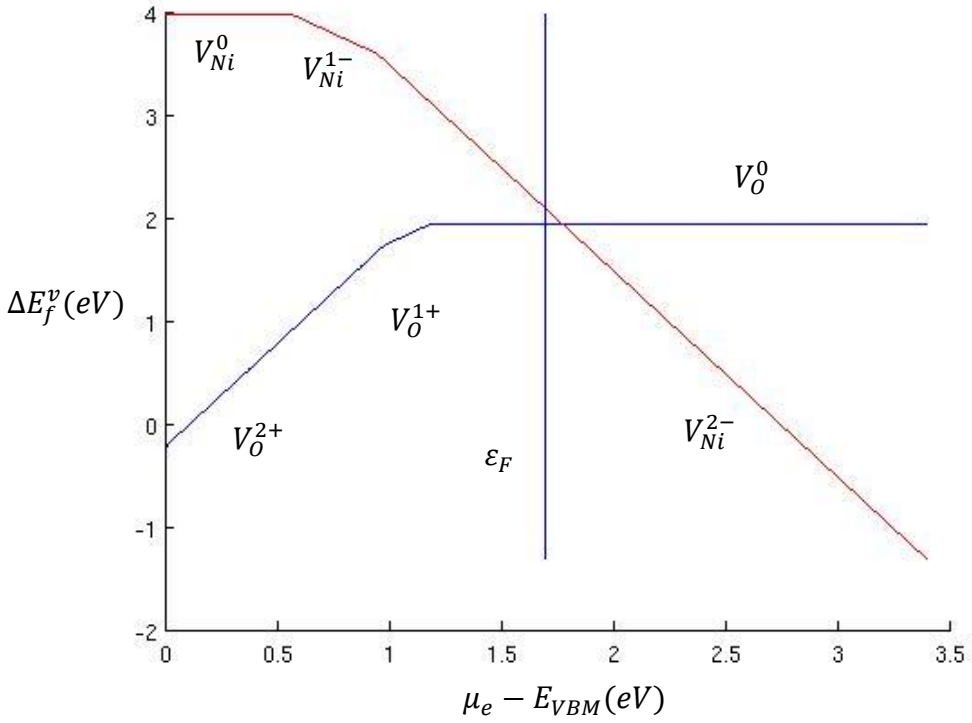

Figure 4. The vacancy formation energy of charged Ni vacancies and charged O vacancies as a function of the Fermi level $\boldsymbol{\varepsilon_F}$ in un-doped NiO crystal at condition of T=1000 K and $\boldsymbol{p_{O_2}}$ =0.2 atm.

Table 2. The calculated result of vacancy formation energy of charged Ni vacancies and charged O vacancies in un-doped NiO crystal at condition of T=1000 K and $\boldsymbol{p_{O_2}}$ =0.2 atm.

vacancies	**Formation energy (DFT+U)**
V_{Ni}^{0}	3.98
V_{Ni}^{1-}	2.86
V_{Ni}^{2-}	2.11
V_{O}^{0}	1.92
V_{O}^{1+}	2.44
V_{O}^{2+}	3.15

3.3 CONCLUSION

The actual concentration of various charged vacancies of Ni vacancies and O vacancies in NiO crystal are major dependent on preparation process and environment of NiO crystal. Our DFT calculation made qualitative prediction. The various charged vacancy formation energies of Ni vacancies and O vacancies in intrinsic NiO crystal will change with temperature and oxygen pressure. At condition of T=1000 K and p_{O_2} =0.2 atm, the most stable vacancies in intrinsic NiO crystal are V_{Ni}^{2-} for Ni vacancies and V_{O}^{0} for O vacancies.

4.0 DIFFUSION PATHS AND BARRIERS OF CHARGED VACANCIES

4.1 COMPUTATION METHOD

Because NiO crystal is antiferromagnetic, there are one elementary path for O atom-vacancy exchange and two distinct elementary paths for Ni atom-vacancy exchange, same spin and reverse spin respectively (shown in Fig.5). For each diffusive jump with different charge states of Ni vacancies and O vacancies, we used the climbing image nudged elastic band method (NEB) [46] to determine the minimum energy path (MEP). Then we applied dimer method to obtain the energies of transition states with higher accuracy and verified the transition state (which should have only one imaginary vibrational mode) with vibrational frequency calculations. Except NEB calculations and the transition state structure of O vacancy with 0 charge (V_O^0) were optimized under constant-volume restriction until the Hellman-Feynman force exerted on each ion is less than 0.05 eV/Å, all other crystal structures were optimized under Hellman-Feynman force limitation of 0.01 eV/Å.

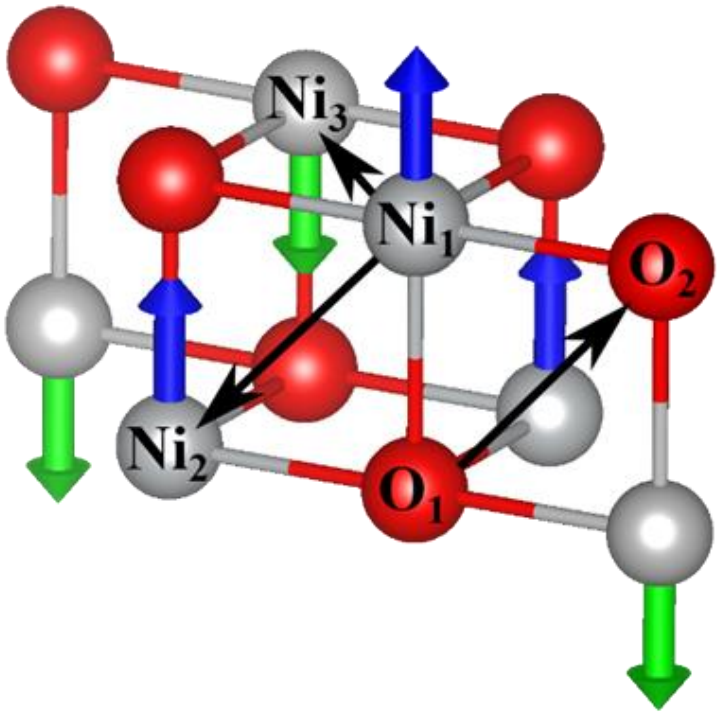

Figure 5. Schematics of various paths (delineated with black arrows) for O vacancy and Ni vacancy to diffuse through the alumina bulk crystal. In the figure, the red balls represent O atoms and the gray balls represent Ni atoms.

4.2 RESULTS AND DISCUSSION

It is worth mentioning that we calculated the energies of transition state of charged Ni vacancies by dimer method with spin initially set to be 0 and -2 respectively which represented spin reversing occurred (spin initially set to be 0) or did not occurred (spin initially set to be -2) at transition state. The result shows that the energy of transition state of Ni vacancies with

spin initially set to be -2 is lower, which means the spin reversing does not occur at transition state.

In addition, we performed another NEB calculation to investigate the possibility of diffusion through tetragonal site of Ni and O vacancies. For O vacancies diffusion and Ni vacancies diffusion on reverse spin path, the tetragonal site is not stable. We tried to calculate the energy of the structure with a tetragonal site atom on the diffusion path for this two situations. But the atom initially placed at tetragonal site would move to vacancy site after relaxation. We even set the initial position of images in NEB for this two situations to let the diffusion go through tetragonal site. But the result showed that the diffusion path would return to linear path, not through tetragonal site. However, for Ni vacancies diffusion on same spin path, the tetragonal site is stable. For V_{Ni}^{0} and V_{Ni}^{1-}, the energy of the structure with tetragonal site atom is lower than the energy of the structure at transition state on linear diffusion path. Then we performed a NEB calculation on tetragonal diffusion path to find the transition state energy and made sure the migration energy of diffusion through tetragonal site was lower than it of diffusion through linear path. While for V_{Ni}^{2-}, the energy of the structure with tetragonal site atom is higher than the energy of the structure at transition state on linear diffusion path. Then we can conclude that for the same spin diffusion path of Ni vacancies, V_{Ni}^{0} and V_{Ni}^{1-} diffused through tetragonal site (shown in Fig. 6) while V_{Ni}^{2-} diffused through almost linear path, not through tetragonal site (shown in Fig. 7). For the reverse spin diffusion path of Ni vacancies (shown in Fig. 8) and all O vacancies (shown in Fig. 9), they diffused through almost linear path, not through tetragonal site. Thus, we calculated the migration energy for each diffusive jump and presented our calculation results in Table 3. We can see from the table that the charge

state of the vacancy strongly influences the vacancy diffusion in NiO crystal, especially for O vacancies.

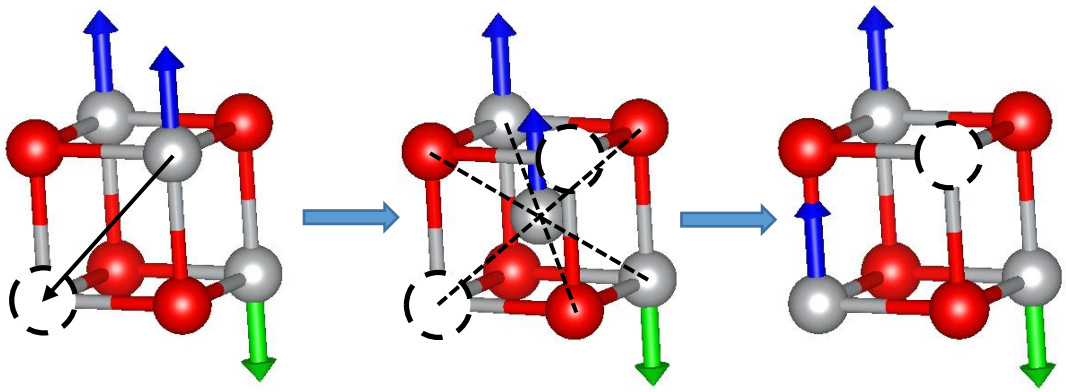

Figure 6. Diffusion path through tetragonal site for $\boldsymbol{V_{\mathrm{Ni}}^{0}}$ and $\boldsymbol{V_{\mathrm{Ni}}^{1-}}$ diffusion.

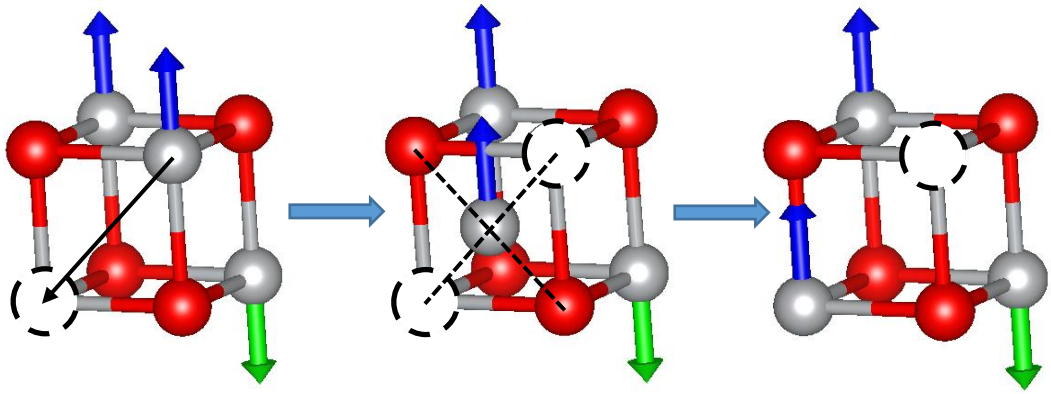

Figure 7. Linear path for same spin $\boldsymbol{V_{\mathrm{Ni}}^{2-}}$ diffusion.

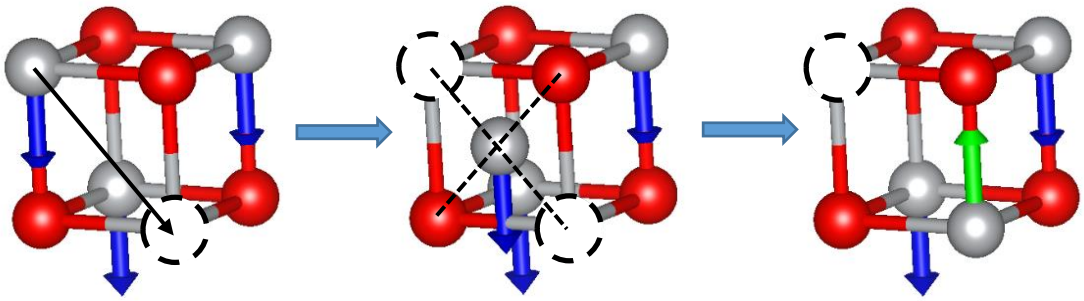

Figure 8. Linear path for reverse spin **Ni** vacancy diffusion.

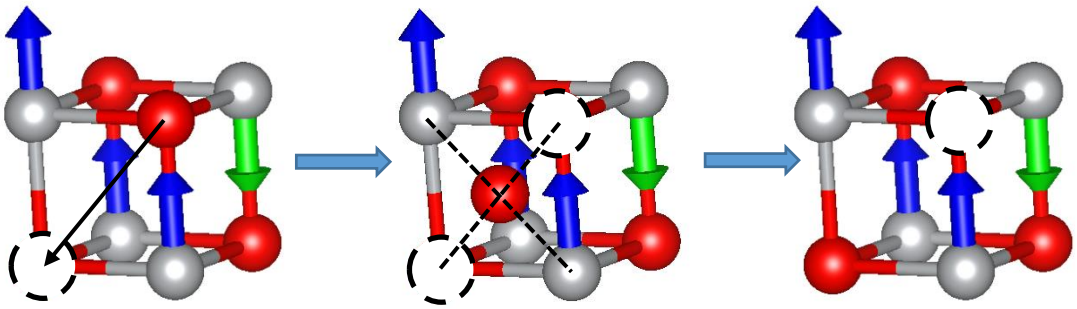

Figure 9. Linear path for **O** vacancy diffusion

Table 3. Calculated migration energy for charged Ni and O vacancy diffusion in NiO. Zero point energy correction is included in the migration energy by calculating the vibrational frequencies of the vacancies and their transition states.

Ni vacancies	**Diffusion barrier (DFT+U same spin)**	**Diffusion barrier (DFT+U reverse spin)**	**Diffusion barrier (experiment)**
V_{Ni}^{0}	1.76	2.53	1.32~2.52 [3, 7, 9]
V_{Ni}^{1-}	1.63	2.02	
V_{Ni}^{2-}	1.84	1.84	

O vacancies	**Diffusion barrier (DFT+U)**	**Diffusion barrier (experiment)**
V_{O}^{0}	4.15	2.21~5.4 [8, 47]
V_{O}^{1+}	3.10	
V_{O}^{2+}	2.23	

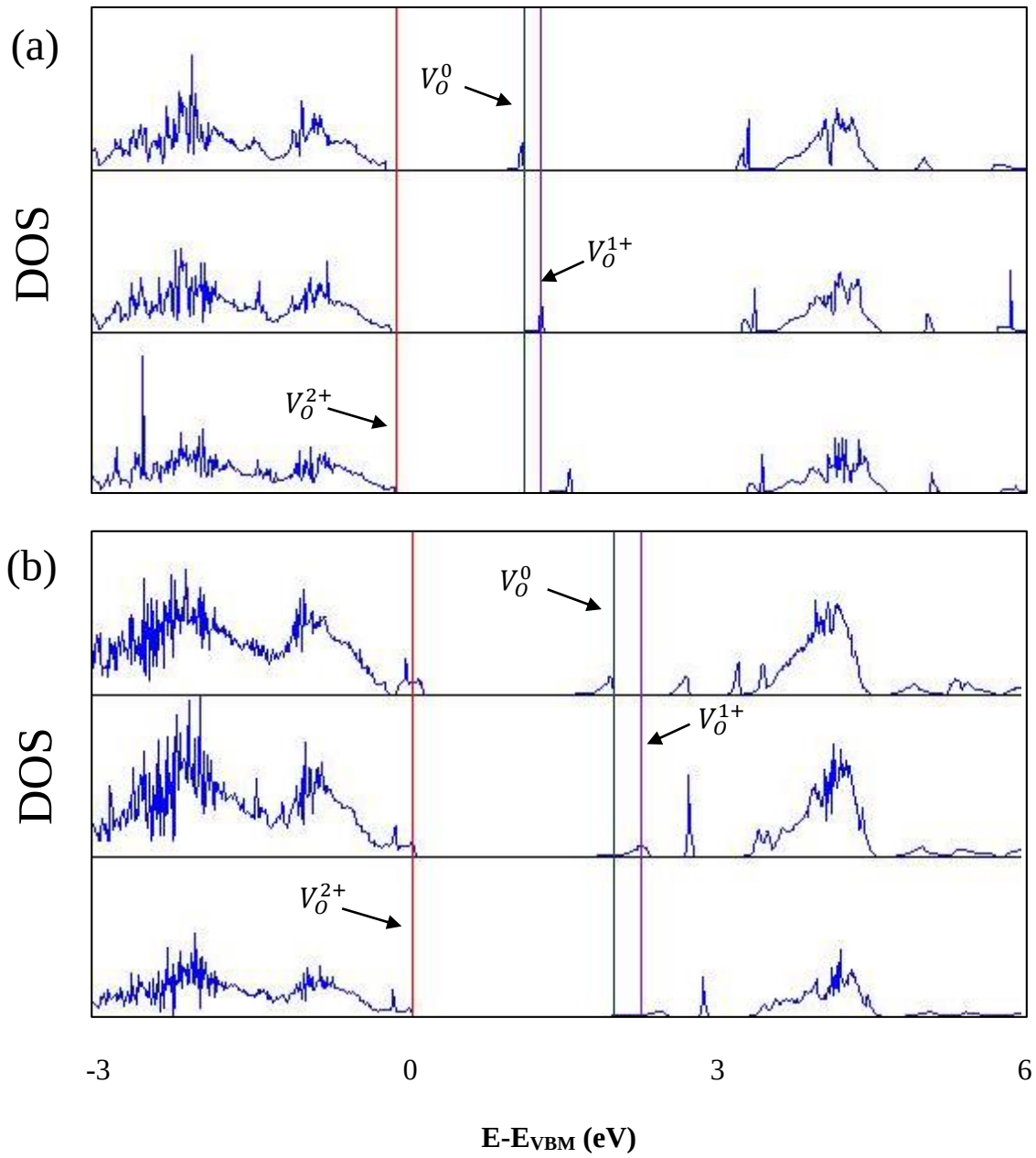

Figure 10. Calculated densities of states (DOS) associated to the defect states of O vacancy in NiO at (a) the relaxed state and (b) the transition state

In order to investigate the physical origin of charge-dependent vacancy diffusion, we analyzed the electron structure of the NiO crystal with charged vacancies at vacancy state and transition state respectively. As shown in Fig. 10, compared to perfect NiO crystal, NiO crystal

with charged vacancies have defect level inside the band gap. We can see that defect level move towards conduct band when O vacancy move from vacancy state to transition state. It is almost same for defect level shift of O vacancies with different charges. Suppose that the migration energy for vacancy diffusion consists of two parts, the total energy change of valence band electrons and the energy change of electrons occupying the defect level in the diffusion process. The total number of valence band electrons does not change with different charge states of the vacancies while the number of electrons occupying defect level varies with different charge states. The number of electrons occupying defect level can be calculated by integrating the DOS from VBM up to maximum occupied energy level [48] as shown in Fig. 10. For O vacancies in NiO crystal, the number of electrons occupying defect level for V_O^0, V_{O}^{1+} and V_{O}^{2+} are 2 , 1 and 0 respectively. Suppose the total energy changes of valence band electrons do not vary with different charges of the O vacancies. Then the difference of migration energies between O vacancies of different charges should be multiple of defect level shift energy and the multiple should be the difference of numbers of electrons occupying the defect level, which can be expressed by the following equation:

$$\Delta E_{\mathrm{m}}^{q'} - \Delta E_{\mathrm{m}}^{q} = (q' - q)\Delta E_{shift} \tag{6}$$

where $\Delta E_{\mathrm{m}}^{q}$ is migration energy for O vacancies with charge q and ΔE_{shift} is the defect level shift energy. As shown in Fig. 11, our result exhibits good linear relation of defect level shift and differences of migration energies as we expect. The slopes of the lines in Fig. 11 are just the numbers of differences in electrons occupying the defect level.

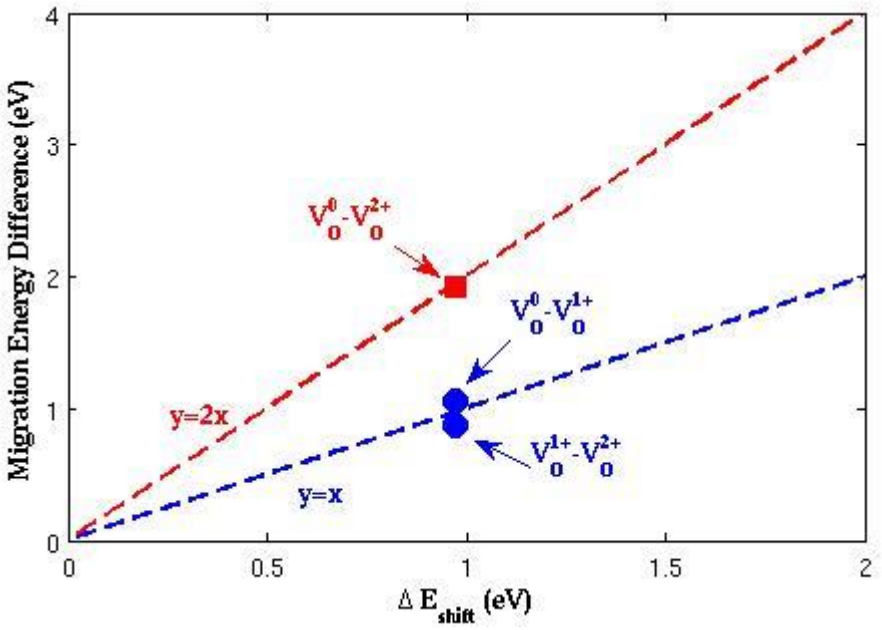

Figure 11. The calculated difference in diffusion migration energy for O vacancies with different charges as a function of the defect level shift energy (ΔE_{shift}). The dashed lines are used to show linear relations with specified slopes.

As for Ni vacancies, the defect level shift is so small that the difference of the total energy change of valence band electrons for vacancies with different charges is comparative to defect level shift (as shown in Fig. 12). Then the total energy change of valence band can not be neglected in intrinsic Ni vacancies. As shown in Table. 3, the migration energies for V_{Ni}^{0}, V_{Ni}^{1-}, V_{Ni}^{2-} with same spin are 1.99 eV, 1.86 eV and 1.84 eV respectively. The migration energies for V_{O}^{0}, V_{O}^{1+}, V_{O}^{2+} are 4.15 eV, 3.10 eV and 2.23 eV respectively. We can see that the differences of migration energies for Ni vacancies with different charges are much smaller than the differences of migration energies for O vacancies. The reason is that the defect level shift of Ni vacancies is much smaller than the defect level shift of O vacancies. This proves the validity of our theory in O vacancy part from another perspective.

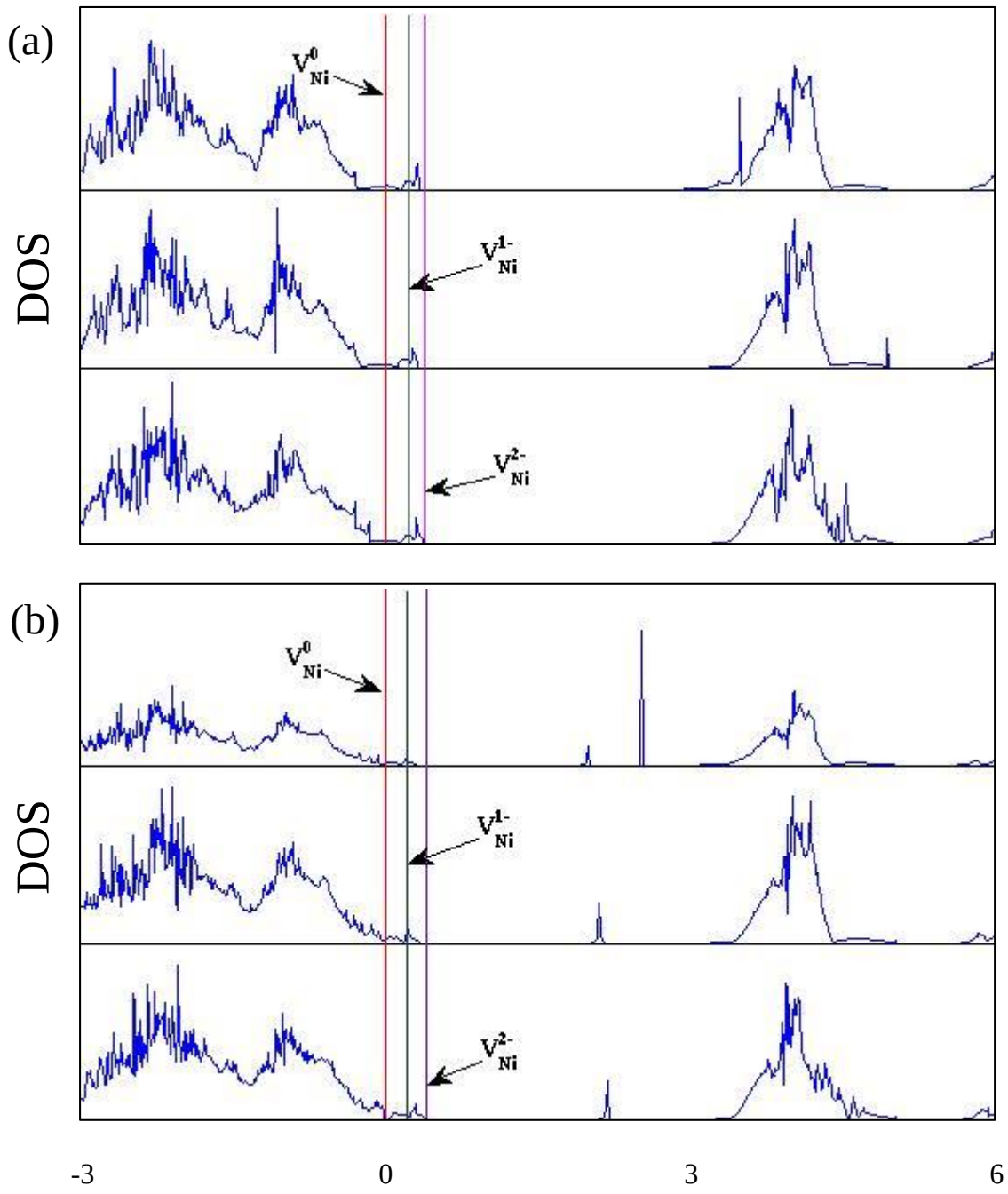

Figure 12. Calculated densities of states (DOS) associated to the defect states of Ni vacancy in NiO at (a) the relaxed state and (b) the transition state (the position of diffusing Ni atoms are placed around mid point along linear diffusion path, not around tetragonal site)

4.3 CONCLUSION

Detailed diffusion paths of various charged Ni vacancies and O vacancies were investigated. Except V_{Ni}^{0} and V_{Ni}^{1-} for same spin diffusion path go through tetragonal site, in all other situations, vacancies go through almost linear path. The calculation result of migration energy of various charged vacancies showed that charge had a dramatic impact on migration energy, especially for O vacancies in NiO.

5.0 KINETIC MONTE CARLO SIMULATION

5.1 COMPUTATION METHOD

Since Ni vacancies have two elementary paths for diffusion, we performed the Kinetic Monte Carlo (KMC) simulations based on the harmonic transition state theory [49] to evaluate the diffusivity of Ni vacancies in NiO crystal between 1200 K and 1700 K.

The main idea of KMC is simulating the time evolution of some processes occurring in nature by using transition rate to repeat random sampling. In this thesis, the rate constant for diffusion can be calculated using a simplified transition state theory by the following equation:

$$k_T = n_p\, v \exp(\frac{-\Delta E_m}{kT}) \tag{7}$$

where n_p is the number of possible jump directions; ν is the harmonic frequency and ΔE_m is the migration energy of this jump. Because there are two diffusion path with different migration energy and different frequency, the rate of two processes can be combined to obtain the total rate and the time step is calculated as inverse of the total rate. At each time step one of the two possible processes is randomly selected with probability that is the product of the time step and the rate of the individual process [50].

In long term, the diffusion distance and diffusion time have the correlation that:

$$t = \frac{x^2}{2D} \tag{8}$$

where t is the diffusion time; x is the diffusion distance and D is the diffusion coefficient. By tracing the vacancies in the KMC simulation, we can obtain the diffusion time t and the diffusion distance x. Then we can fit the diffusion coefficient D.

According to Arrhenius Law:

$$D = f \exp(-\Delta E/kT) \quad (1)$$

using the diffusion coefficient D simulated by KMC from 1200K to 1700K, we can fit the effective migration energy ΔE.

5.2 RESULTS AND DISCUSSION

From the Arrhenius plot (as shown in Fig. 13, an example of V_{Ni}^{0}) of our calculated diffusion coefficients, we predicted that the effective migration energy for the Ni diffusion through exchanges with V_{Ni}^{0}, V_{Ni}^{1-} and V_{Ni}^{2-} were 2.16 eV, 1.89 eV and 1.84 eV, respectively.

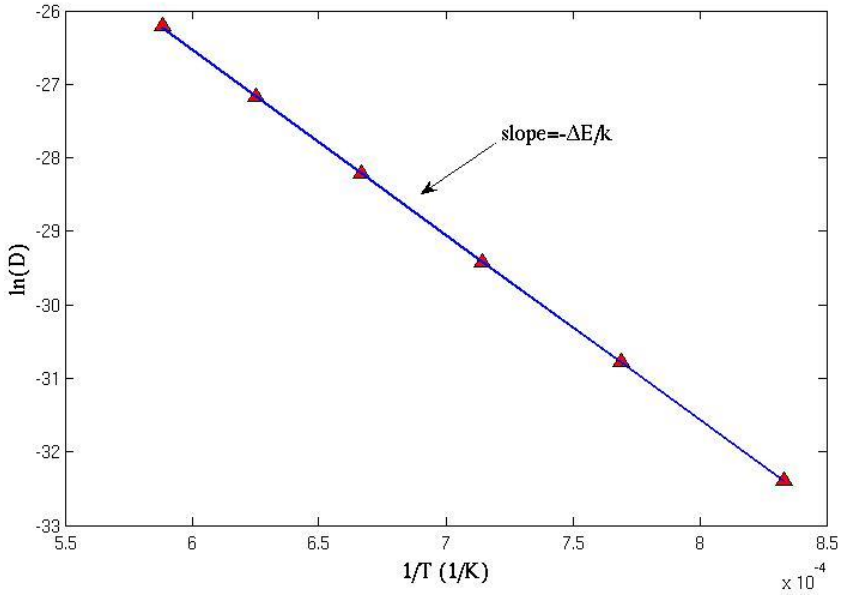

Figure 13. Arrhenius plot of ln(D) of $\boldsymbol{V_{\mathrm{Ni}}^{0}}$ as a function of 1/T to fit $\boldsymbol{\Delta E}$. $\boldsymbol{k}$ is Boltzmann constant.

We can see that the migration energy of V_{Ni}^{0} is much higher than it of V_{Ni}^{1-} and V_{Ni}^{2-}. These results agree with the conclusion in Peterson's work [9] that V_{Ni}^{2-} moves with the smaller activation enthalpy than V_{Ni}^{1-}. In summary, we found that V_{Ni}^{2-} led to the fastest diffusion of Ni in NiO crystal.

6.0 CONCLUSION

In this thesis, we presented our result of the formation energy and migration energy of Ni vacancies and O vacancies with different charge states in intrinsic NiO crystal calculated by DFT+U. Detailed diffusion paths for charged vacancies in NiO crystal are investigated. We predicted migration energy of vacancy diffusion varied with charge states of the vacancies, especially for O vacancies in NiO. Further analysis reveals that defect level shift and different number of electrons on defect level contributes to migration energy difference for different charged vacancies. This work provides a view on controlling diffusion kinetics by tuning charge states of the vacancies or changing defect level shift through some processes such as doping.

BIBLIOGRAPHY

[1] P. Kritzer, N. Boukis, and E. Dinjus, "Review of the corrosion of nickel-based alloys and stainless steels in strongly oxidizing pressurized high-temperature solutions at subcritical and supercritical temperatures," *Corrosion,* vol. 56, pp. 1093-104, 11/ 2000.

[2] T. Oshima, Y. Yamaguchi, and K. Kuroda, "Microstructural characterization of oxide scale formed by early stage of oxidation of 17%Cr-Mn-Ni austenitic stainless steel," in *Sixth Pacific Rim International Conference on Advanced Materials and Processing, 5-9 Nov. 2007*, Switzerland, 2007, pp. 99-102.

[3] A. Atkinson and R. I. Taylor, "The self-diffusion of Ni in NiO and its relevance to the oxidation of Ni," *Journal of Materials Science,* vol. 13, pp. 427-32, 02/ 1978.

[4] P. Kofstad, *Nonstoichiometry, diffusion and electrical conductivity in binary metal oxides*. Chichester, Sussex, UK: Wiley-Interscience, 1972.

[5] S. P. Mitoff, "Electrical conductivity and thermodynamic equilibrium in nickel oxide," *Journal of Chemical Physics,* vol. 35, pp. 882-889, 1961.

[6] C. M. Osburn and R. W. Vest, "Defect structure and electrical properties of Nio—II. Temperatures below equilibration," *Journal of Physics and Chemistry of Solids,* vol. 32, pp. 1343-1354, // 1971.

[7] M. T. Shim and W. J. Moore, "Diffusion of nickel in nickel oxide," *Journal of Chemical Physics,* vol. 26, pp. 802-804, 04/ 1957.

[8] M. Meyer, S. Barbezat, C. El Houch, and R. Talon, "Diffusion study of oxygen implanted in nickel oxide," in *Third Europhysics Topical Conference, Lattice Defects in Ionic Crystals, 17-21 Sept. 1979*, France, 1980, pp. 6-327.

[9] N. L. Peterson and C. L. Wiley, "Point defects and diffusion in NiO," *Journal of the Physics and Chemistry of Solids,* vol. 46, pp. 43-52, / 1985.

[10] G. J. Koel and P. J. Gellings, "CONTRIBUTION OF DIFFERENT TYPES OF POINT DEFECTS TO DIFFUSION IN CoO AND NiO DURING OXIDATION OF THE METALS," *Oxidation of Metals,* vol. 5, pp. 185-203, 1972.

[11] R. Farhi and G. Petot-Ervas, "THERMODYNAMIC STUDY OF POINT DEFECTS IN SINGLE CRYSTALLINE NICKEL OXIDE: ANALYSIS OF EXPERIMENTAL RESULTS," vol. 39, pp. 1175-1179, 1978.

[12] J. B. Price and J. B. Wagner, Jr., "Determination of the chemical diffusion coefficients in single crystals of CoO and NiO," *Zeitschrift fur Physikalische Chemie, Neue Folge*, vol. 49, pp. 257-270, 05/ 1966.

[13] R. Lindner and Å. Åkerström, "Diffusion of nickel-63 in nickel oxide (NiO)," *Discuss. Faraday Soc.*, vol. 23, pp. 133-136, 1957.

[14] M. L. Volpe and J. Reddy, "Cation self-diffusion and semiconductivity in NiO," *Journal of Chemical Physics*, vol. 53, pp. 1117-25, 08/01 1969.

[15] A. Atkinson, A. E. Hughes, and A. Hammou, "The self-diffusion of Ni in undoped and Al-doped NiO single crystals," *Philosophical Magazine A (Physics of Condensed Matter, Defects and Mechanical Properties)*, vol. 43, pp. 1071-91, 05/ 1981.

[16] A. Atkinson and R. I. Taylor, "The diffusion of 63Ni along grain boundaries in nickel oxide," *Philosophical Magazine A (Physics of Condensed Matter, Defects and Mechanical Properties)*, vol. 43, pp. 979-98, 04/ 1981.

[17] B. Sadigh, T. J. Lenosky, S. K. Theiss, M. J. Caturla, T. Diaz de la Rubia, and M. A. Foad, "Mechanism of boron diffusion in silicon: an ab initio and kinetic Monte Carlo study," *Physical Review Letters*, vol. 83, pp. 4341-4, 11/22 1999.

[18] D. H. Wells Jr, W. N. Delgass, and K. T. Thomson, "Evidence of Defect-Promoted Reactivity for Epoxidation of Propylene in Titanosilicate (TS-1) Catalysts: A DFT Study," *Journal of the American Chemical Society*, vol. 126, pp. 2956-2962, 2004.

[19] S. L. Mielke, D. Troya, S. Zhang, J. L. Li, S. Xiao, R. Car, *et al.*, "The role of vacancy defects and holes in the fracture of carbon nanotubes," *Chemical Physics Letters*, vol. 390, pp. 413-20, 06/01 2004.

[20] M. H. N. Assadi and D. A. H. Hanaor, "Theoretical study on copper's energetics and magnetism in TiO2 polymorphs," *Journal of Applied Physics*, vol. 113, p. 233913 (5 pp.), 06/21 2013.

[21] D. S. Sholl and J. A. Steckel, *Density Functional Theory: A Practical Introduction*. New Jersey: John Wiley and Sons, 2009.

[22] P. Hohenberg and W. Kohn, "Inhomogeneous Electron Gas," *Physical Review*, vol. 136, pp. B864-B871, 11/09/ 1964.

[23] R. O. Jones and O. Gunnarsson, "The density functional formalism, its applications and prospects," *Reviews of Modern Physics*, vol. 61, pp. 689-746, 07/01/ 1989.

[24] J. P. Perdew and Y. Wang, "Pair-distribution function and its coupling-constant average for the spin-polarized electron gas," *Physical Review B (Condensed Matter),* vol. 46, pp. 12947-54, 11/15 1992.

[25] V. N. Staroverov, G. E. Scuseria, J. Tao, and J. P. Perdew, "Tests of a ladder of density functionals for bulk solids and surfaces," *Physical Review B,* vol. 69, p. 075102, 02/13/ 2004.

[26] G. I. Csonka, J. P. Perdew, A. Ruzsinszky, P. H. T. Philipsen, S. Lebègue, J. Paier, *et al.*, "Assessing the performance of recent density functionals for bulk solids," *Physical Review B,* vol. 79, p. 155107, 04/10/ 2009.

[27] J. Harl, L. Schimka, and G. Kresse, "Assessing the quality of the random phase approximation for lattice constants and atomization energies of solids," *Physical Review B,* vol. 81, p. 115126, 03/17/ 2010.

[28] J. P. Perdew, K. Burke, and M. Ernzerhof, "Generalized gradient approximation made simple," *Physical Review Letters,* vol. 77, pp. 3865-8, 10/28 1996.

[29] J. P. Perdew and Y. Wang, "Accurate and simple analytic representation of the electron-gas correlation energy," *Physical Review B,* vol. 45, pp. 13244-13249, 06/15/ 1992.

[30] A. I. Liechtenstein, V. I. Anisimov, and J. Zaanen, "Density-functional theory and strong interactions: Orbital ordering in Mott-Hubbard insulators," *Physical Review B,* vol. 52, pp. R5467-R5470, 08/15/ 1995.

[31] S. L. Dudarev, G. A. Botton, S. Y. Savrasov, C. J. Humphreys, and A. P. Sutton, "Electron-energy-loss spectra and the structural stability of nickel oxide: An LSDA+U study," *Physical Review B,* vol. 57, pp. 1505-1509, 01/15/ 1998.

[32] A. Jain, G. Hautier, S. P. Ong, C. J. Moore, C. C. Fischer, K. A. Persson, *et al.*, "Formation enthalpies by mixing GGA and GGA $+$ U calculations," *Physical Review B,* vol. 84, p. 045115, 07/12/ 2011.

[33] N. J. Mosey and E. A. Carter, "Ab initio evaluation of Coulomb and exchange parameters for DFT+U calculations," *Physical Review B,* vol. 76, p. 155123, 10/25/ 2007.

[34] G. Kresse and D. Joubert, "From ultrasoft pseudopotentials to the projector augmented-wave method," *Physical Review B (Condensed Matter),* vol. 59, pp. 1758-75, 01/15 1999.

[35] G. Kresse and J. Hafner, "Ab initio molecular dynamics for liquid metals," *Physical Review B (Condensed Matter),* vol. 47, pp. 558-61, 01/01 1993.

[36] G. Kresse and J. Furthmuller, "Efficiency of ab-initio total energy calculations for metals and semiconductors using a plane-wave basis set," *Computational Materials Science,* vol. 6, pp. 15-50, 07/ 1996.

[37] H. J. Monkhorst and J. D. Pack, "Special points for Brillouin-zone integrations," *Physical Review B (Solid State),* vol. 13, pp. 5188-92, 06/15 1976.

[38] W. Lei, T. Maxisch, and G. Ceder, "Oxidation energies of transition metal oxides within the GGA+U framework," *Physical Review B (Condensed Matter and Materials Physics),* vol. 73, pp. 195107-1, 05/15 2006.

[39] N. D. M. Hine, K. Frensch, W. M. C. Foulkes, and M. W. Finnis, "Supercell size scaling of density functional theory formation energies of charged defects," *Physical Review B (Condensed Matter and Materials Physics),* vol. 79, p. 024112 (13 pp.), 01/01 2009.

[40] H. P. Komsa, T. T. Rantala, and A. Pasquarello, "Finite-size supercell correction schemes for charged defect calculations," *Physical Review B (Condensed Matter and Materials Physics),* vol. 86, p. 045112 (16 pp.), 07/15 2012.

[41] *CRC handbook of chemistry and physics. 69th edition*: CRC Press, 1988-1989.

[42] F. Tran, P. Blaha, K. Schwarz, and P. Novak, "Hybrid exchange-correlation energy functionals for strongly correlated electrons: applications to transition-metal monoxides," *Physical Review B (Condensed Matter and Materials Physics),* vol. 74, pp. 155108-1, 10/15 2006.

[43] G. A. Sawatzky and J. W. Allen, "Magnitude and origin of the band gap in NiO," *Physical Review Letters,* vol. 53, pp. 2339-42, 12/10 1984.

[44] T. D. Kang, H. S. Lee, and H. Lee, "Optical Properties of Black NiO and CoO Single Crystals Studied with Spectroscopic Ellipsometry," *Korean Physical Society,* vol. 50, p. 632~637, 2007.

[45] P. S. Patil and L. D. Kadam, "Preparation and characterization of spray pyrolyzed nickel oxide (NiO) thin films," *Applied Surface Science,* vol. 199, pp. 211-21, 10/30 2002.

[46] G. Henkelman, B. P. Uberuaga, and H. Jonsson, "A climbing image nudged elastic band method for finding saddle points and minimum energy paths," *Journal of Chemical Physics,* vol. 113, pp. 9901-4, 12/08 2000.

[47] M. Okeeffe and W. J. Moore, "Diffusion of oxygen in single crystals of nickel oxide," *Journal of Physical Chemistry,* vol. 65, pp. 1438-1439, 08/ 1961.

[48] Y. Lei and G. Wang, "Linking diffusion kinetics to defect electronic structure in metal oxides: Charge-dependent vacancy diffusion in alumina," *Scripta Materialia,* vol. 101, pp. 20-23, 2015.

[49] G. H. Vineyard, "Frequency factors and isotope effects in solid state rate processes," *Journal of Physics and Chemistry of Solids,* vol. 3, pp. 121-127, 1957/01/01 1957.

[50] A. F. Voter, "Classically exact overlayer dynamics: Diffusion of rhodium clusters on Rh(100)," *Physical Review B,* vol. 34, pp. 6819-6829, 11/15/ 1986.